Supplemental Information for:
DNA Strand-Displacement Timer Circuits

Joshua Fern[†], Dominic Scalise[†], Angelo Cangialosi[†], Dylan Howie[†], Leo Potters[†] and Rebecca Schulman[†‡]

†Chemical and Biomolecular Engineering, and ‡Computer Science, Johns Hopkins University, Baltimore, MD 21218, United States

SI 0: Materials and Methods

The timer circuit was designed following the principles outlined in Supp. Reference 1. Sequences for each domain were drawn from Table S1 of the Supporting Online Material for Supp. Reference 1 and are listed here in Table 1. Domains *S6* and *S5* listed below correspond to Domains *1* and *2* depicted in Figure 2 of the Main Text and Supp. Figure 0. The toehold (*t*) domain of System 2 was designed to have minimal non-specific interactions with the sequences of both systems using NUPACK.[2] Domain Names and Sequences are listed 5' to 3'. Additional schematics of the DNA complexes and the reactions are shown in SI 2.

Table 1: Sequence Data

Strand Names	Domain Names	Sequences
Source 1 Top	*S6 t S5*	CA TAACACAATCA CA TCT CA CCACCAAACTT CA
Source 1 Bottom	*t' S6'*	TG AGA TG TGATTGTGTTA TG
Initiator 1	*S6 t*	CA TAACACAATCA CA TCT CA
Delay 1 Top	*S5*	CA CCACCAAACTT CA CT
Delay 1 Bottom	*S5' t' S6' (2nt)*	AG TG AAGTTTGGTGG TG AGA TG TG
Reporter 1 Top	*S5 t Quencher*	CA CCACCAAACTT CA TCT CA/3IABkFQ/
Reporter 1 Bottom	*FAM t' S5' t'*	/56-FAM/TG AGA TG AAGTTTGGTGG TG AGA TG
Reporter 1 Full Complement	*t S5 t*	CA TCT CA CCACCAAACTT CA TCT CA
Source 2 Top	*S27 t S28*	AC AACACTCTATT AC AAT AC TCTACAATTCA AC
Source 2 Bottom	*t' S27'*	GT ATT GT AATAGAGTGTT GT
Initiator 2	*S27 t*	AC AACACTCTATT AC AAT AC
Delay 2 Top	*S28*	AC TCTACAATTCA AC CA
Delay 2 Bottom	*S28' t' S27' (2nt)*	TG GT TGAATTGTAGA GT ATT GT AA
Reporter 2 Top	*S28 t Quencher*	AC TCTACAATTCA AC AAT AC/3IABRQSp/
Reporter 2 Bottom	*TexasRed t' S28' t'*	/5TexRd-XN/GT ATT GT TGAATTGTAGA GT ATT GT
Reporter 2 Full Complement	*t S28 t*	AC AAT AC TCTACAATTCA AC AAT AC

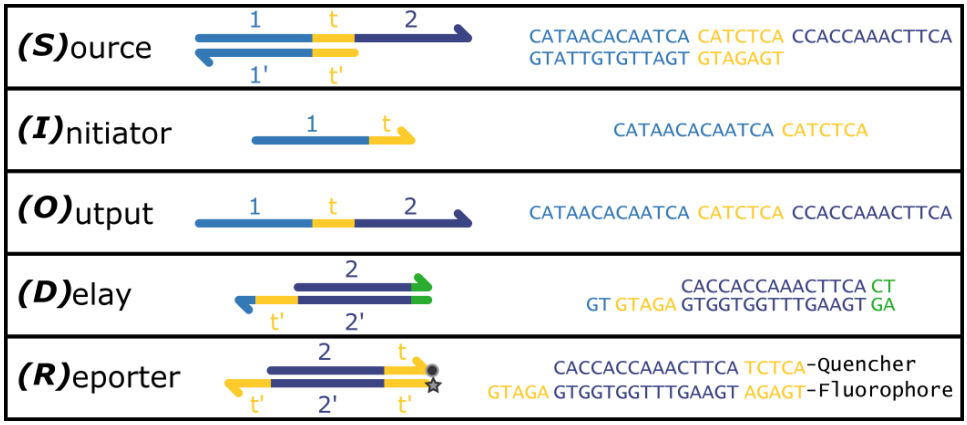

Supplemental Figure 0: Schematic of reaction species with their sequences as listed in Table 1. Reactions between species for the timer circuit are shown in Supp. Figures 3 and 6.

Sequences were ordered as lyophilized powder from Integrated DNA Technologies (IDT). The **Reporter Top** and **Reporter Bottom** strands were ordered purified by high-performance liquid chromatography (HPLC) and all other strands were ordered impure with standard desalting. Strands were suspended in Millipore purified water to a concentration of ~1 mM and stored at -20°C. Empirical oligonucleotide stock concentrations were determined by assaying the absorbance (OD260) of 1000x diluted samples of each stock solution at 260 nm. The extinction coefficient provided by IDT was used to calculate stock concentrations using the Beer-Lambert law.

Source, **Delay** and **Reporter** complexes were prepared at a concentration of 100 μM in Tris-acetate-EDTA buffer with 12.5 mM Mg^{++} (1x TAE/Mg^{++}). Each complex was annealed in an Eppendorf Mastercycler PCR by holding the solutions at 90°C for 5 minutes followed by cooling at -1°C per minute down to 20°C. After annealing, the **Source** complexes were incubated with 100 μM of their complementary **Initiator** strand overnight at room temperature to react with any poorly formed **Source** complexes. The **Source** complex was not incubated with any other strands or complexes due to the increased complexity of gel purification.

After annealing each complex and incubating the **Source** complexes overnight, all complexes were purified by polyacrylamide gel electrophoreses (PAGE). Ten percent polyacrylamide gels were cast by mixing 3.25 mL of 19:1 40% acrylamide/bis solution (Bio-Rad) with 1.3 mL 10x TAE/Mg^{++} and 8.45 mL Millipore-purified H_2O. This solution was polymerized by the addition of 78 μL 10% ammonium persulfate (APS) and 5.4 μL tetramethylenediamine (TEMED) in a gel cassette with a large single well comb at the top of each gel. Fifteen percent polyacrylamide gels were prepared in a similar fashion except with a corresponding higher fractional volume of 40% acrylamide/bis stock solution. Two hundred microliters of annealed DNA complexes were mixed with 6x loading dye (New England Biolabs, product #B7021S) and loaded into the wells of the gels in a Scie Plas TV100K cooled vertical electrophoresis chamber. The gels were run at 150V and 4°C for 1.5 or 3 hours for 10% and 15% polyacrylamide gels. **Reporter** and **Delay** complexes were purified using 10% gels and the **Source** complex was purified using 15% gels. After running for the appropriate time, the bands were cut out using UV-shadowing at 254 nm for visualization. Bands were diced into ~1 mm^3 pieces, mixed with 500 μL of 1x TAE/Mg^{++} buffer and were shaken on a vortexer overnight at room temperature. The DNA solutions were then transferred by pipet to a fresh tube leaving behind the gel pieces. The solutions were centrifuged for 5 minutes at 3000x*g* to precipitate any remaining gel pieces. The DNA solutions were transferred to a new tube and stored at 4°C until use. The concentrations of these purified complexes were then measured with an Eppendorf Biophotometer with a dilution factor of 30x using the approximate extinction coefficient (ε):

$$\varepsilon_{\text{Final}} = \varepsilon_{Top-strand} + \varepsilon_{Bottom-strand} - 3200N_{AT} - 2000N_{GC}$$

where *N* indicates the number of hybridized A-T or G-C pairs in each complex.[3]

Reaction kinetics were measured on quantitative PCR (qPCR) machines (Agilent Stratagene Mx3000 and Mx3005 series) at 25°C. Reactions were prepared in 96-well plates using 150 μL/well volumes. Each well contained 1x TAE/Mg^{++} and 2 μM $PolyT_{20}$ strands to help displace reactant species from the pipet tips used to add species and potentially from the well walls. In a typical experiment, Millipore-purified H_2O, TAE/Mg^{++} and $PolyT_{20}$ strands were first mixed together. **Reporter** complexes were then added at 100 nM for System 1 or 200 nM for System 2.

Baseline fluorescent measurements of the **Reporter** complex alone was conducted for each experiment for 0.5 to 1 hour with measurements every 1 to 10 minutes. This baseline was taken to be where the [**Output**] is equal to zero as detected by the **Reporter** and was subtracted from all subsequent data. After measuring this baseline, DNA strands or complexes were added to each well, depending on the experiment (see SI 1-4). Fluorescence measurements were taken every 1-5 minutes for Delay characterization or every 5-10 minutes for Production characterization and Timer experiments.

SI 1: Reporter Calibration

The **Reporter** complex (Figure 2c in Main Text) was used to indirectly measure the concentration of the single-stranded **Output** strands in solution as a function of time. A **Reporter** that reacts reversibly with the **Output** species was used as an irreversible reporter could compete with the **Delay** species. The reporter follows the reaction:

$$Reporter + Output \underset{k_r}{\overset{k_f}{\rightleftharpoons}} \text{Fluorophore} + \text{Quencher} \qquad \text{(SI-Eqn. 1)}$$

where the quencher-modified top strand of the **Reporter** complex is displaced by an invading strand causing in increase of fluorescence. The forward reaction rate constant, k_f, is expected to be around 5×10^4 $M^{-1}s^{-1}$.[4] Two calibrations were conducted to translate measured fluorescence intensities to levels of free **Output** concentration for each experiment. It was assumed that the measured fluorescence was proportional to the concentration of unquenched fluorophore, [**Fluoro.**] (*e.g. Fluorophore* in SI-Eqn. 1), through a proportionality constant α. To determine α, we measured the fluorescence of the **Reporter** complex with known concentrations of the **full complement** (**FC**) to the bottom strand of the **Reporter** (see Table 1) and measured the change in fluorescence before and after addition of the complementary strand (Supp. Figure 1). In general, we used the equation

$$[FC] = \alpha * \Delta\text{Fluorescence} + \beta \qquad \text{(SI-Eqn. 2)}$$

for [**FC**] equal to 0, 25, 50, 75 and 100 nM. In the ideal case, β is equal to zero. Alpha was determined by calculating the slope after fitting a line to [**FC**] vs. ΔFluorescence (Supp. Figure 1). This calibration enables the normalization of all fluorescence data into [**Fluoro.**]. Additionally, Supp. Figure 1 shows that photobleaching of the fluorophores are not a significant factor in measuring fluorescence as seen by the stable, non-decreasing intensity values.

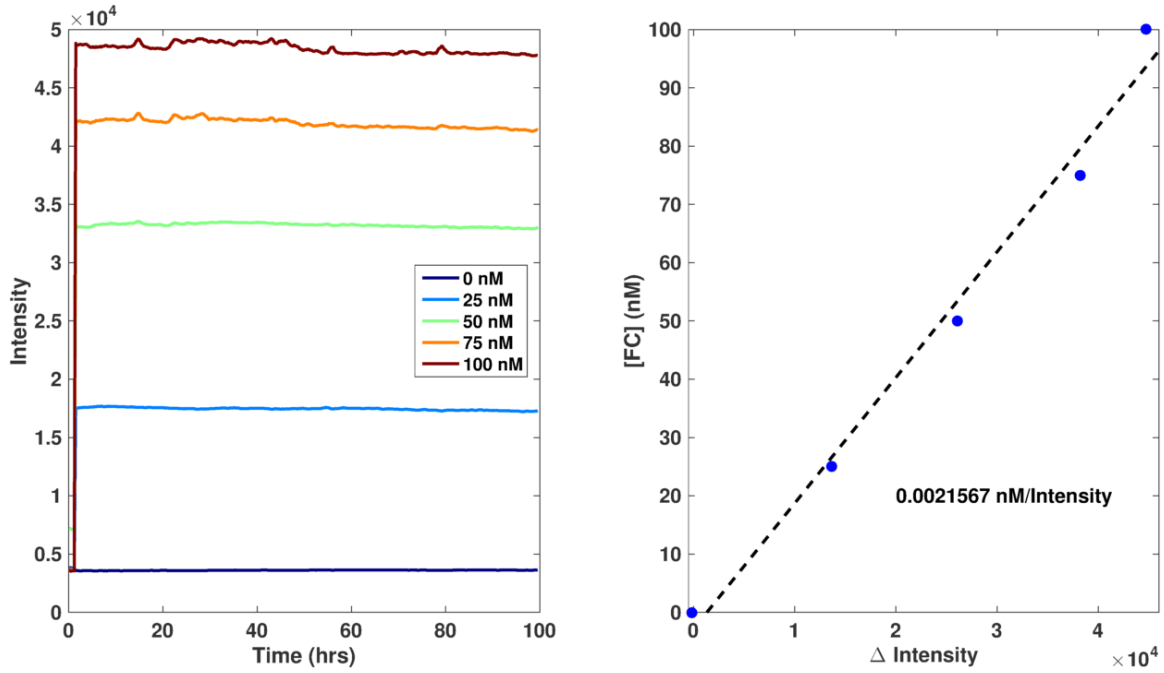

Supplemental Figure 1: Example calibration plots for the **Reporter** complex with its full complement to convert raw intensity values into [**Fluoro.**]. **FC** was added to 100 nM **Reporter** at concentrations ranging from 0 – 100 nM as noted in the legend.

To convert the [**Fluoro.**] into [**Output**], the K_{eq} for the reporter reaction shown in SI-Eqn. 1 was calculated by mixing the **Reporter** complex with known concentrations of **Output** strand and using the equation:

$$K_{eq} = \frac{[Fluoro.]\text{^}2}{([O]_0 - [Fluoro.])([R]_0 - [Fluoro.])} \qquad \text{(SI-Eqn. 3)}$$

where $[O]_0$ is the concentration of **Output** (*e.g.* 25, 50, 75 or 100 nM) added to the **Reporter** solution and $[R]_0$ is the initial **Reporter** complex concentration (*e.g.* 100 nM). In general, we found that the intensities measured with this calibration method decreased over the duration of the experiment (Supp. Fig. 2a), possibly due to **Reporter** complexes becoming stuck in the "off" state. Due to this decrease, the K_{eq} was calculated as a function of time. The data was segmented into 75 bins (~1.3 hours each), with each bin having a K_{eq} calculated as the average K_{eq} over the [**Output**] tested (Supp. Fig. 2b,c).

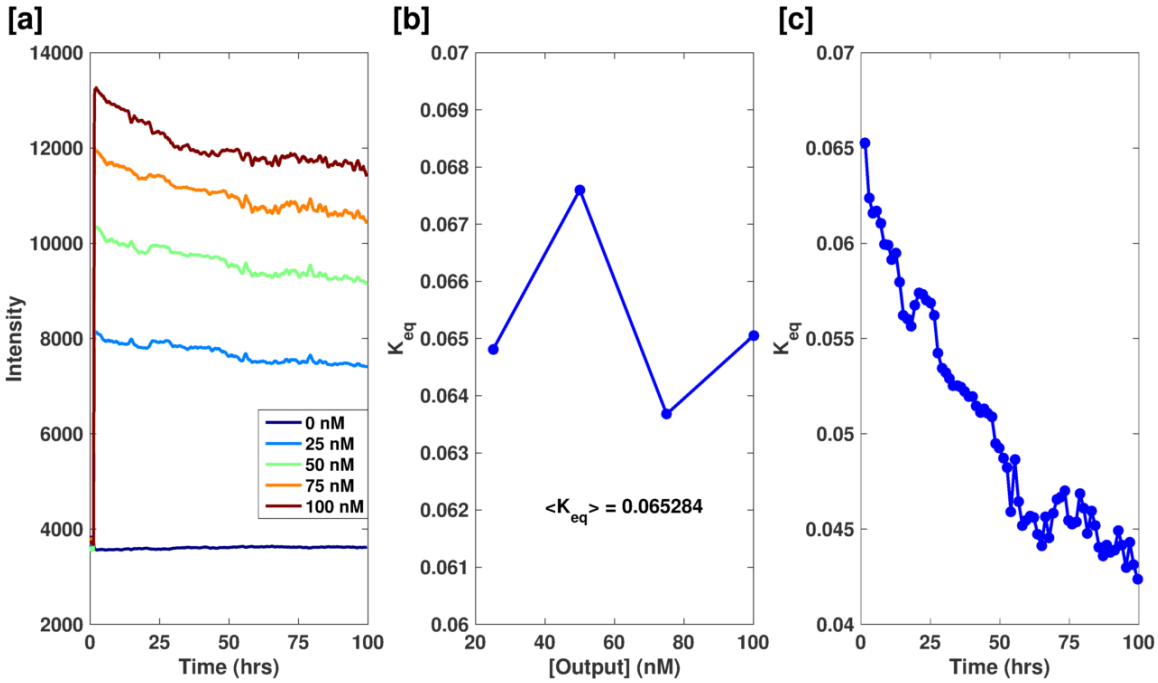

Supplemental Figure 2: Example calibration plots for the **Reporter** complex with **Output** to convert [**Fluoro.**] values into [**Output**]. (a) **Output** was added to 100 nM **Reporter** at concentrations ranging from 0 – 100 nM as noted in the legend. (b) For each time segment, the K_{eq} was calculated as the average value over the [**Output**]'s tested. Little variance was seen between the K_{eq}'s calculated at each [**O**] within a given time segment. The initial segment is shown (t = 1 hr). (c) The K_{eq} decreases as a function of time. Each segment usually contained 1.3-1.5 hours of data.

The concentration of **Fluoro.** was then converted into [**Output**] through the equation

$$[O] = \frac{[Fluoro.]^2}{K_{eq}([R]_0 - [Fluoro.])} + [Fluoro.] \qquad \text{(SI-Eqn. 4)}$$

where *[Fluoro.]*, *[O]* and K_{eq} are functions of time. This equation reports the total concentration of **Output** as the sum of free **O** in solution and **O** that is transiently bound to the **Reporter** complex.

SI 2: Production and Delay Reaction Characterization

To understand the timer system, we initially characterized the production reaction (between the **Source** and **Initiator** molecules) without a concurrent delay reaction. Multiple production reactions using various concentrations of **Initiator** and **Source** were conducted to calculate the forward and reverse reaction rate constants for the set of reactions shown in Supp. Figure 3. Two sets of reactions were conducted: [**S**]=[**I**] and [**S**]x[**I**]=1. In the first case, the production rate (k_{prod}) varies because the product of the initial concentrations of **Initiator** and **Source** is changing. In the second case, the production rate is theoretically constant between experiments on "short" time scales.

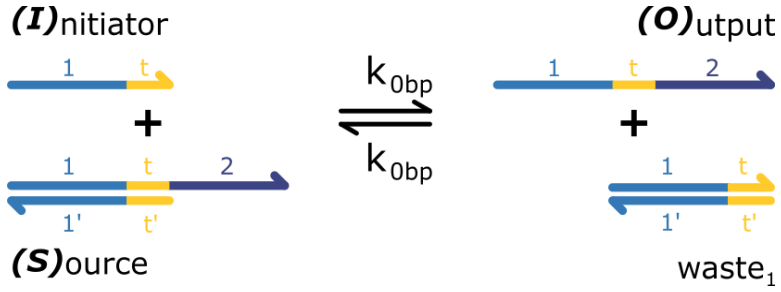

Supplemental Figure 3: Schematic for the Production circuit. The **Initiator** reacts with the **Source** complex through a fraying mechanism at the ends of the double-stranded regions to produce **Output** and **waste**$_1$. The forward and reverse reaction rate constant depend on DNA sequence and the point of strand-displacement initialization and thus could be different values, but for simplicity a single rate constant, k_{0bp}, was chosen.

The **Source** and **Reporter** were incubated for about 6 hours until the measured intensity reached a steady state prior to the addition of **I**. This steady state intensity is thought to be a small population of free **Output** left over from the purification process, although interactions between the **Source** and **Reporter** complexes may exist. The concentration of detected **Output** by the **Reporter** corresponded to 0.01-0.02x[**Source**] used in each experiment (Supp. Figure 4).

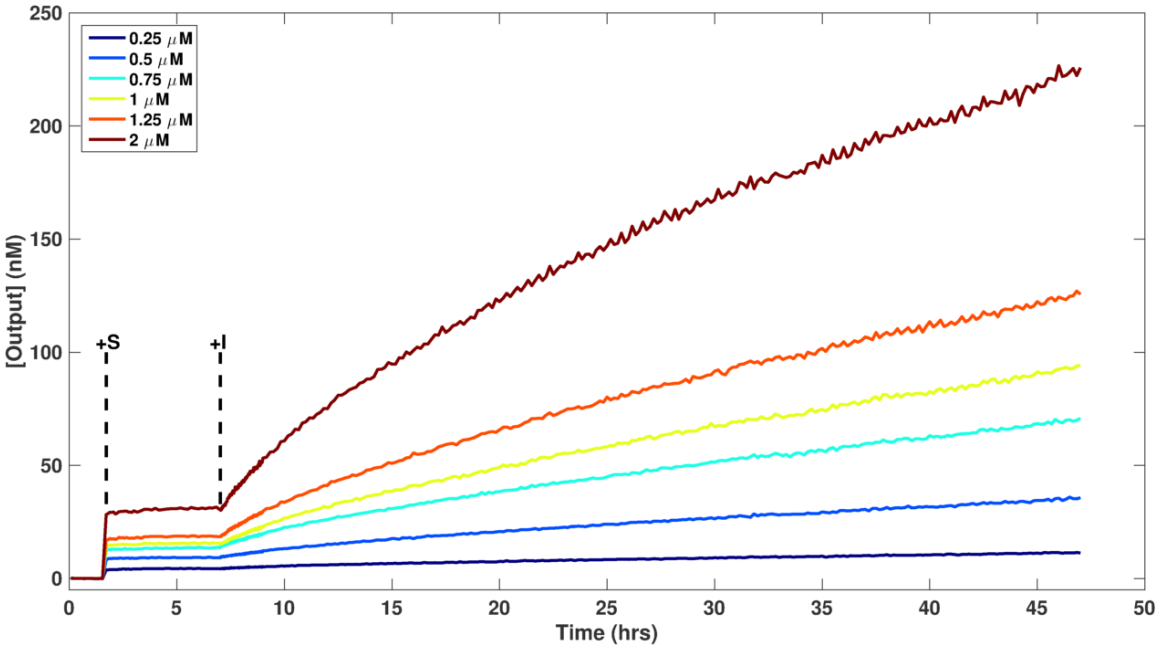

Supplemental Figure 4: Characterization of the effect of [**Source**] and [**Initiator**] on the observed release of **Output**. The **Source** is mixed with the **Reporter** after 1.5 hours and incubated for about 6 hours, when the **Initiator** is added (denoted by black dashed lines). For the curves shown, [**S**] is equal to [**I**] and is shown in the legend. The concentration of initial **Output** detected prior to initiation scales with the amount of [**S**] added. Data is identical to that shown in Supp. Figure 5a and Main Text Figure 3a.

The post-initiation reaction curves were fit using MATLAB to initially calculate k_{0bp} for this set of reactions using the second-order reaction kinetics equation:

$$\frac{d[O]}{dt} = k_{0bp}[I][S] - k_{0bp}[O][waste_1] \quad \text{(SI-Eqn. 5)}$$

The **Reporter** reaction was not included in the fitting procedure because its equilibration kinetics were assumed to be much faster (~10^5x faster reaction rate constant) than that of the Production reaction. However, the reaction rate constants calculated from this model did not capture the dynamics seen in Supp. Fig 5a-b - *i.e.* a quick release of **O** followed by a slower, more linear region. We hypothesized that this was due to a small concentration of **Source** that reacted quickly and irreversibly with the **Initiator** present in the reaction volumes, perhaps because of errors in sequence produced during solid state DNA synthesis. We call this small population $[\mathbf{S}]_{Leak}$ which reacts with reaction rate constant k_{Leak}. To account for this possibility, we used the following equation to generate a better fit to the experimental data:

$$\frac{d[O]}{dt} = k_{0bp}[I][S] - k_{0bp}[O][waste_1] + k_{Leak}[S]_{Leak}[I]$$

and to calculate the model parameters k_{0bp}, k_{Leak} and $[\mathbf{S}]_{Leak}$. Additional information regarding $\mathbf{S}_{Leak}$ can be found in SI 6. An example of such a fit is shown in Supp. Figure 5c and the fit parameters are compiled in Table 2. The average k_{0bp} was 0.49±0.13 1/M-sec which is in good agreement with the reported value of 0.5 1/M-sec.[4] $[\mathbf{S}]_{Leak,0}$ varied from 0.5 to 4.7% of $[\mathbf{S}]_0$.

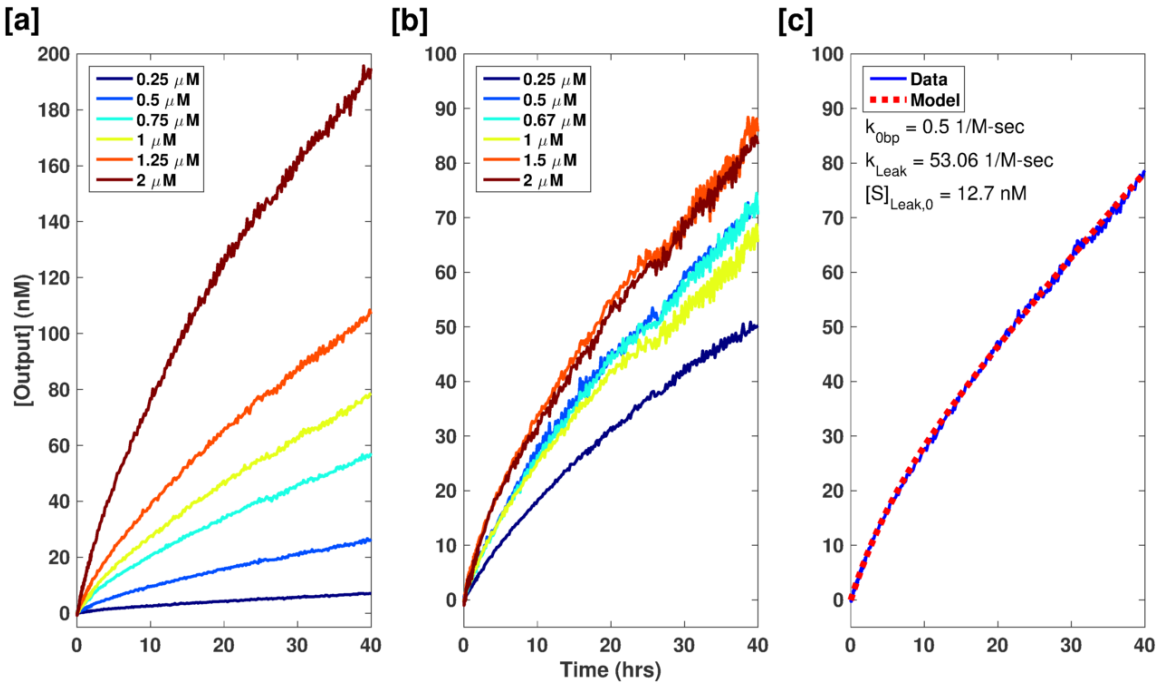

Supplemental Figure 5: Characterization of Production reactions. Production reactions were measured for [**Source**] = [**Initiator**] in the range of 0.25-2 μM (a) and for [**S**] x [**I**] = 1 (b). The legend in (b) shows the concentration of **Source** in the reaction mixture. (c) Example comparison between experimental measurements and the model resulting from the fit of reaction rate constants for [**S**]=[**I**]=1 μM. Reaction curves were fit using a bimolecular reaction kinetics model to calculate a second-order reaction rate constant. Reaction rate constants for each curve are listed below in Table 2.

As shown in Supp. Figure 5a, the production rate varied with the concentrations of **Source** and **Initiator**. From Equation 5 in the Main Text, the production rate is expected to follow a power law ($k_{Prod} \sim [\boldsymbol{S}]_0^2$) when initial concentrations of **S** and **I** are equal. The experimentally determined production rate increased to the exponential of 1.6 with increasing **S** and **I** instead of 2. There was also a small variation in the production rate for the case [**S**]x[**I**]=1, where the initial k_{prod} was expected to be constant among the reaction conditions tested (see Table 2). The deviation from the expected result in both cases could be due to other undesired reactions present in between reaction species.

Table 2: Reaction rate constants for the Production reactions shown in Supp. Figure 5. The production rate constant (k_{prod}) was calculated using Equation 5 listed in the Main Text using the initial concentrations of **Source** and **Initiator**. Values listed are result of fit with 95% confidence interval bounds. Overall values are the average and standard deviation of all rows (k_{0bp}) or rows in the [**S**]x[**I**]=1 set of experiments (k_{prod}).

Experiment Type	[S] (μM)	[I] (μM)	k_{0bp} (1/M-sec)	k_{prod} (nM/hr)	k_{Leak} (1/M-sec)	$[S]_{Leak}$ (nM)
[S]=[I]	0.25	0.25	0.676±0.008	0.152±0.002	336±20	1.3±0.1
	0.5	0.5	0.645±0.006	0.58±0.005	129±7	4.6±0.2
	0.75	0.75	0.647±0.004	1.311±0.009	91±4	8.8±0.2
	1	1	0.501±0.004	1.803±0.014	53±2	12.7±0.4
	1.25	1.25	0.439±0.004	2.47±0.021	43±2	19.0±0.6
	2	2	0.279±0.005	4.016±0.066	20±1	53.8±2.0
[S]x[I]=1	0.25	4	0.32±0.01	1.14±0.02	8±1	11.7±0.8
	0.5	2	0.46±0.01	1.67±0.02	27±2	13.2±0.6
	0.67	1.5	0.46±0.01	1.65±0.02	35±3	12.6±0.6
	1	1	0.39±0.01	1.41±0.03	52±4	14.1±0.7
	1.5	0.67	0.53±0.01	1.91±0.03	96±6	18.2±0.8
	2	0.5	0.55±0.01	1.97±0.02	129±7	15.9±0.6
Overall			0.5±0.1	1.6±0.3		

The Delay circuit module was characterized by the degree to which the **Delay** complex was able to sequester free **Output**. The kinetics of the reaction between **Delay** and **Output** was too fast to capture using the concentration ranges tested in order to fit reaction rate constants for the set of reactions show in Supp. Figure 6. The Delay reaction is slightly reversible due to 2 extra bases on the **Delay** complex that are not complementary to the **Output** (shown in green). These bases are important for decreasing undesired reactions between the **Source** and **Delay** complexes, whose reaction rate constant is on the same order as the Production circuit (initialized *via* fraying). However, this reaction set is expected to be very forward reaction dominated since $k_{forward}$ ~2x10^6 1/M-sec and $k_{reverse}$ ~10^2 1/M-sec.[4]

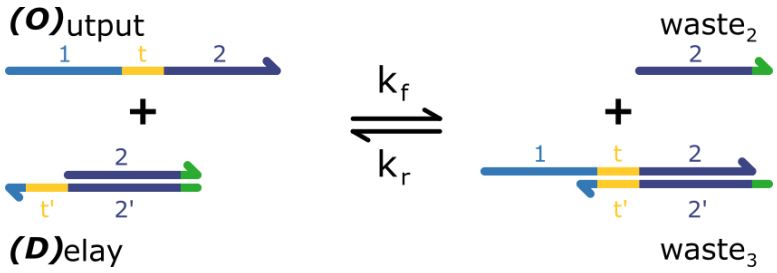

Supplemental Figure 6: Schematic for the Delay circuit. The **Output** reacts with the **Delay** complex through a 7 base-pair toehold to produce two waste species. Two extra bases on the **Delay** complex (shown in green) inhibit a leak reaction between **Source** and **Delay** complexes.

Two sets of experiments were run to investigate whether the **Delay** complex efficiently sequestered **Output** in a reaction solution. The first set was run by adding **D** at various concentrations to the **Reporter** followed by the addition of **O**. As shown in Supp. Fig. 7a, the concentration of **O** detected closely matched the expected result: [**O**] = [**O**]$_0$-[**D**]. The second set of experiments was run by first adding **O** to the **Reporter** followed by the addition of **D**, leading to a sudden decrease in fluorescence intensity and detected free **O** (Supp. Fig. 7b). Again the remaining [**O**] matched the expected concentrations determined by the amount of **D** added. The concentration of **O** remaining when the **D** exceeded the initial concentration of **O** added did not fully decrease to zero due to the reversibility of the Delay reaction (Supp. Fig. 6).

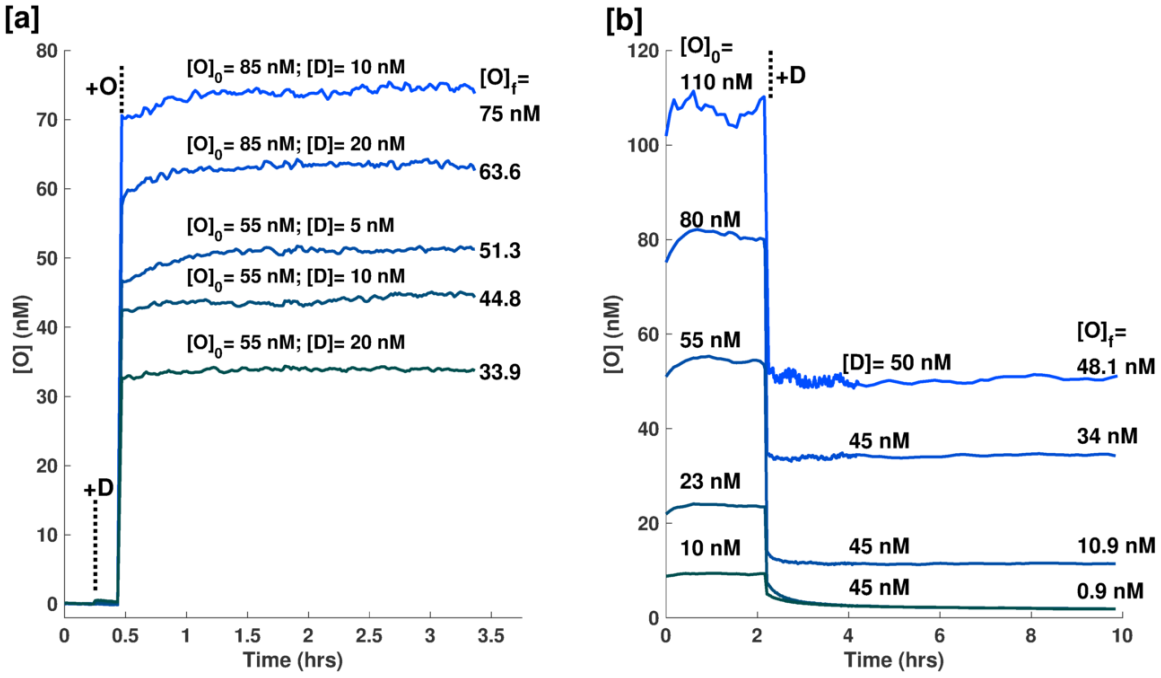

Supplemental Figure 7: Characterization of the Delay circuit. (a) **O** is added to **R** and **D** leading to a rise in detected **O** by the **Reporter**. Black dashed lines indicate the times **D** or **O** is added to the **Reporter** solution. The concentration of **O** and **D** added to each reaction mixture is annotated above each trace. [**O**]$_f$ is the average [**O**] over the last 30 data points. (b) **D** is added to **Reporter** and **O** leading to a decrease in fluorescence as **O** is being sequestered by **D**. The data in Fig. 3b of the Main Text is calculated from the data shown here in (a) and (b).

SI 3: Timer Experiments with System 1

Timer experiments were conducted similar to Production experiments, except both **Source** and **Delay** were mixed with the **Reporter** after the initial baseline was measured (~1 hour). **Initiator** was mixed into the wells after the intensity reached a steady-state, at about 22-24 hours. Both **S** and **I** were kept equal in these experiments. From Table 2, [**S**]=[**I**]=1 µM produces **Output** at ~1.8 nM/hr, [**S**]=[**I**]=0.5 µM at ~0.6 nM/hr and [**S**]=[**I**]=0.25 µM at ~0.15 nM/hr (Fig. 3c-d in the Main Text and Supp. Figs. 8-10).

The delay time (t_{Delay}) was determined by calculating a moving linear fit of each curve post-**Initiator** addition. The span of each fit included 100 or 60 data points, depending on the reaction conditions. The step size was ½ of the span in each case (50 and 30 points). The x-intercept from the fit with the largest slope was chosen as the delay time. Other algorithms (*e.g.* the time [**O**] or d[**O**]/dt surpasses a specified value) gave similar time delays, but were more sensitive to noise/bias.

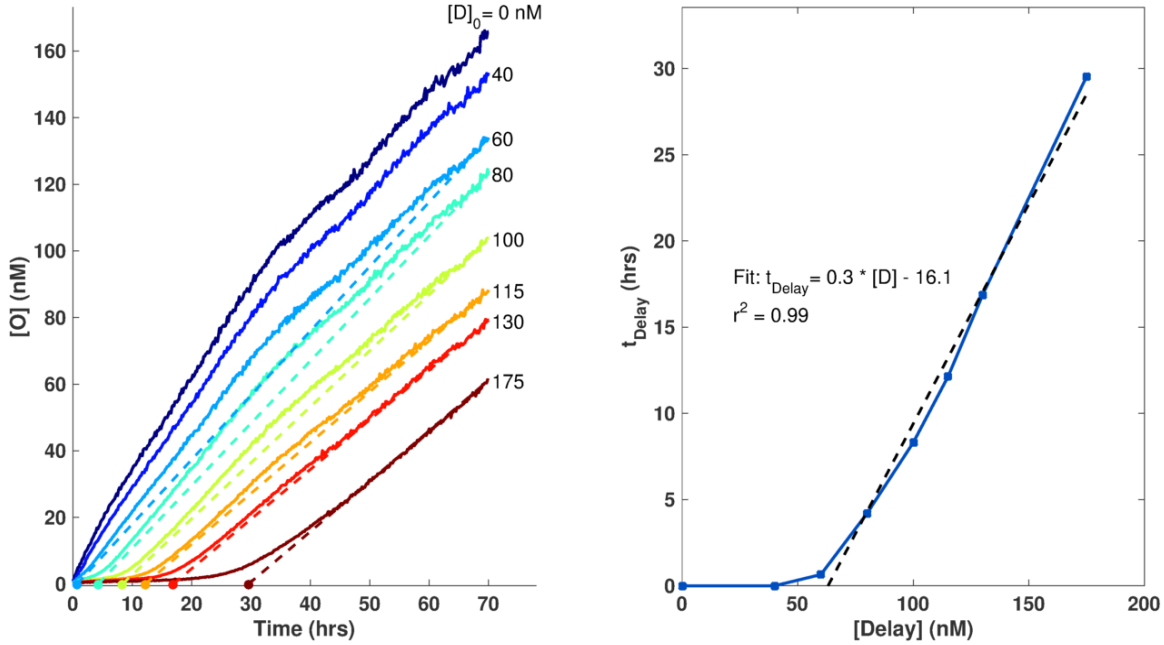

Supplemental Figure 8: [**Output**] *vs.* time and t_{delay} *vs.* [**Delay**] for reactions using [**S**]=[**I**]=1 µM production conditions for System 1. Dashed lines in the left plot are guides showing the calculated time delay. Dashed line in the right plot shows a linear fit for points with t_{Delay} greater than zero. Data is the same as in Figure 3c,d of the Main Text.

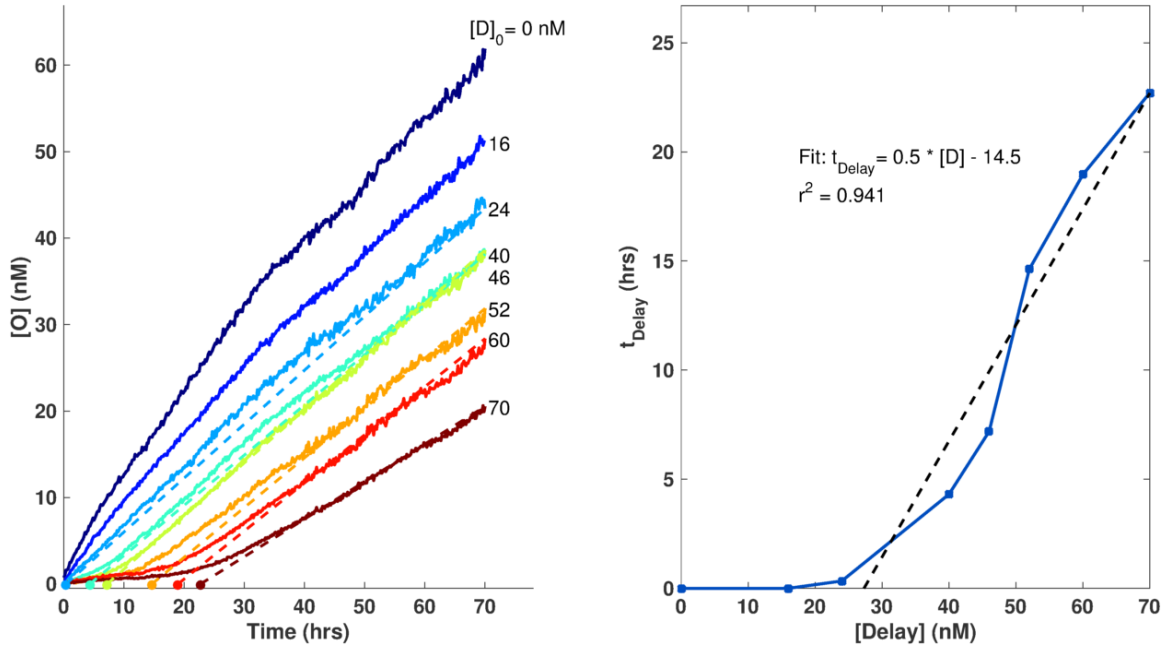

Supplemental Figure 9: [**Output**] *vs.* time and t_{delay} *vs.* [**Delay**] for reactions using [**S**]=[**I**]=0.5 µM production conditions for System 1. Dashed lines in the left plot are guides showing the calculated time delay. Dashed line in the right plot shows a linear fit for points with t_{Delay} greater than zero.

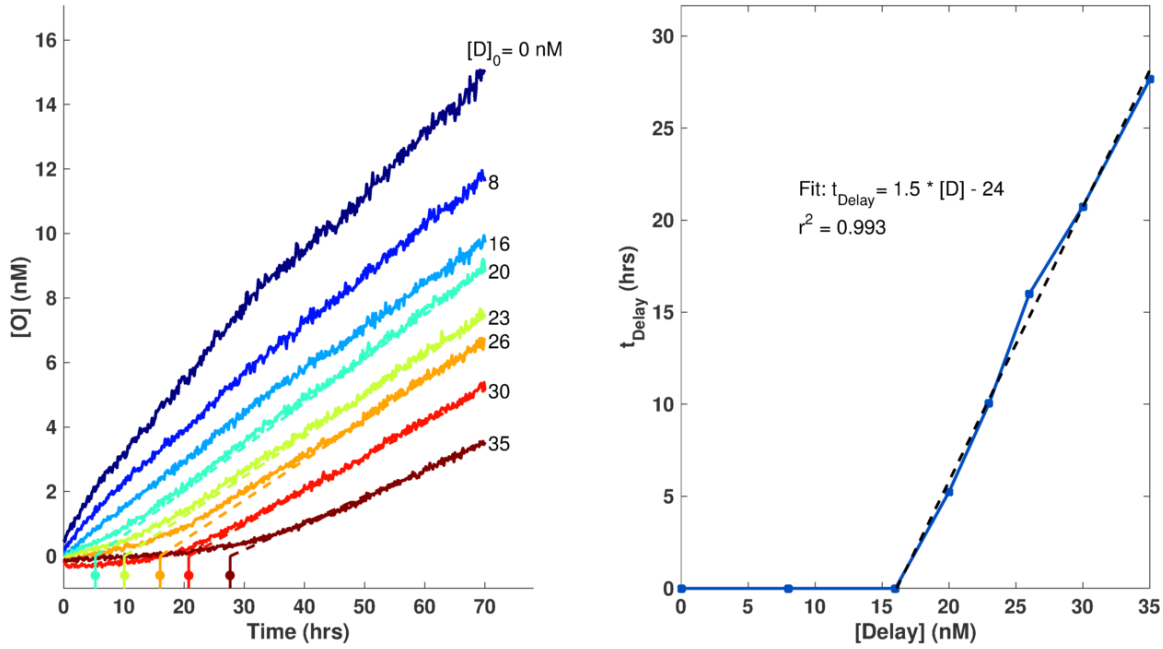

Supplemental Figure 10: [**Output**] *vs.* time and t_{delay} *vs.* [**Delay**] for reactions using [**S**]=[**I**]=0.25 µM production conditions for System 1. Dashed lines in the left plot are guides showing the calculated time delay. Dashed line in the right plot shows a linear fit for points with t_{Delay} greater than zero.

The rate of production (d[**O**]/dt) was calculated for each reaction condition. The slope of each curve was calculated as the average over the last 90 data points (15 hours). We found that the production rate at that time point decreased slightly as a function of [**Delay**], possibly due to the uncharacterized reactions mentioned elsewhere. Despite the **Delay** dependent effects observed, an appropriate [**Delay**] can be chosen from a desired production rate and time delay using Table 2 and Supp. Figure 11.

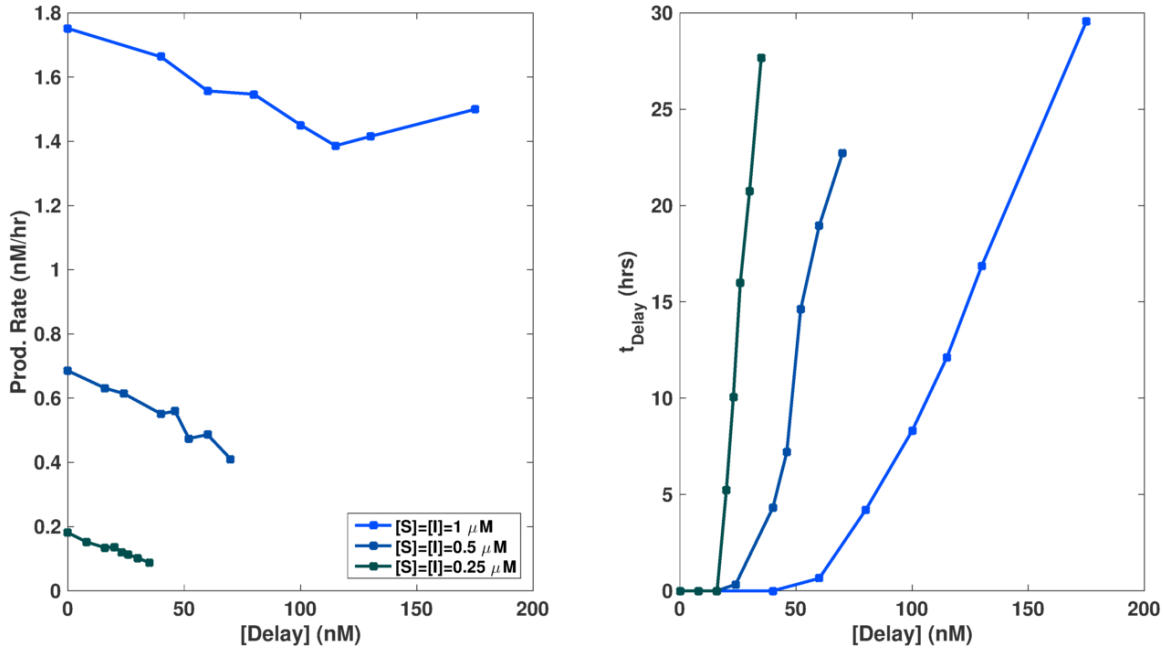

Supplemental Figure 11: Production rate *vs.* [**Delay**] and t_{delay} *vs.* [**Delay**] for System 1. Production rate was calculated as the average over the last 90 data points (15 hours). Production rate decreases with [**Delay**] due to possible undesired reactions between circuit components.

SI 4: Timer Experiments with System 2

Experiments for System 2 were conducted the same as with System 1 except with a [**Reporter**] of 200 nM. **Output** production from System 2 was found to be slower than with System 1 (Supp. Figures 12-14). This could be due to DNA sequence differences between the systems; notably the toehold domain of System 2 is expected to have weaker binding than that of System 1 because it has less G-C base content. The 7bp toehold of the **Delay** complex is weaker as well. Additionally, if there are significant interactions between the **Source** or **Delay** and the **Reporter** complex, the increased **Reporter** concentration could be an attributing factor. Finally, while System 1 had a decrease in production rate with increasing [**Delay**], System 2 showed an increase in production rate (Supp. Figure 15).

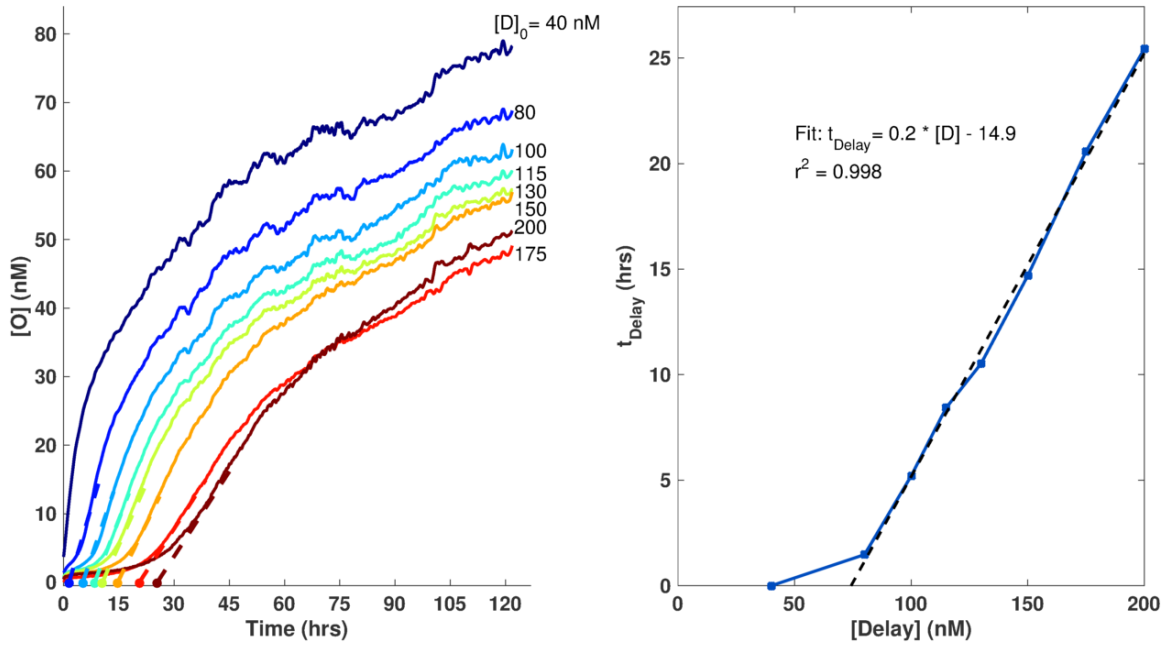

Supplemental Figure 12: [**Output**] *vs.* time and t_{delay} *vs.* [**Delay**] for reactions using [**S**]=[**I**]=1 µM production conditions for System 2. Dashed lines in the left plot are guides showing the calculated time delay. Dashed line in the right plot shows a linear fit for points with t_{Delay} greater than zero.

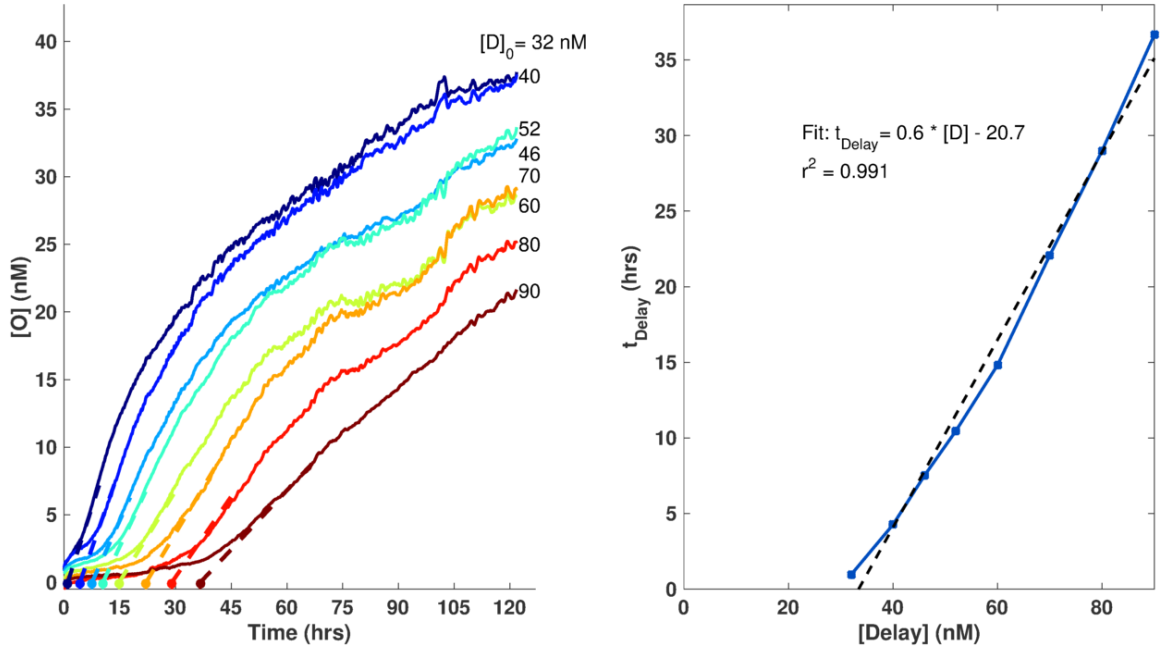

Supplemental Figure 13: [**Output**] *vs.* time and t_{delay} *vs.* [**Delay**] for reactions using [**S**]=[**I**]=0.5 µM production conditions for System 2. Dashed lines in the left plot are guides showing the calculated time delay. Dashed line in the right plot shows a linear fit for points with t_{Delay} greater than zero.

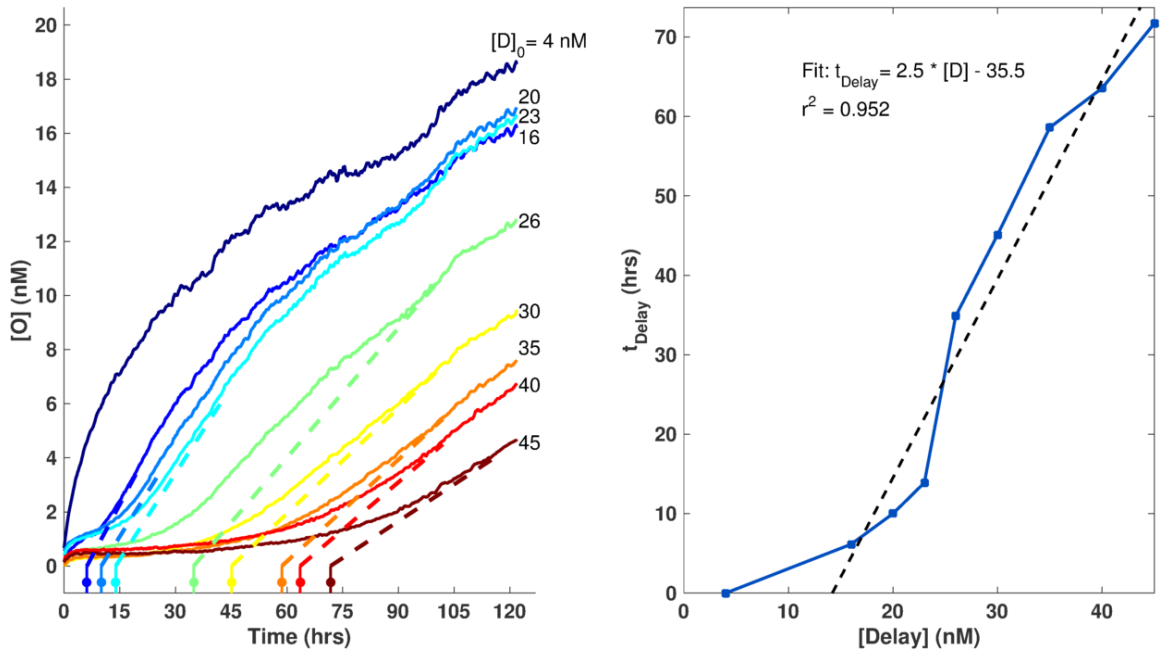

Supplemental Figure 14: [**Output**] *vs.* time and t_{delay} *vs.* [**Delay**] for reactions using [**S**]=[**I**]=0.25 μM production conditions for System 2. Dashed lines in the left plot are guides showing the calculated time delay. Dashed line in the right plot shows a linear fit for points with t_{Delay} greater than zero.

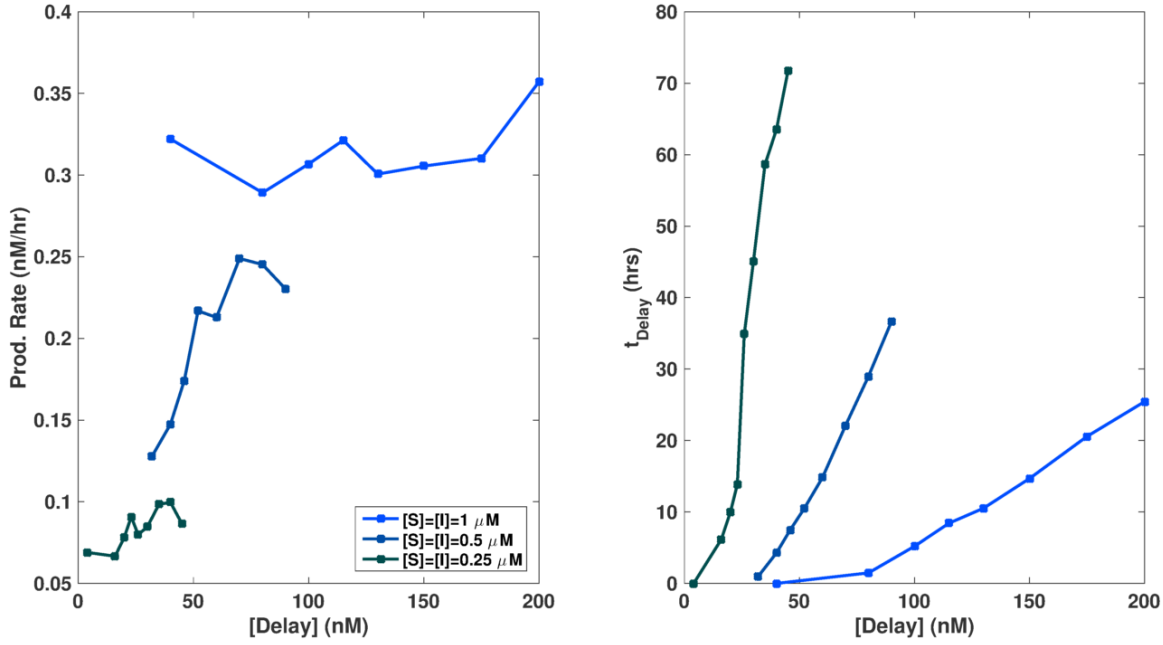

Supplemental Figure 15: Production rate *vs.* [**Delay**] and t_{delay} *vs.* [**Delay**] for System 2. Production rate was calculated as the average over the last 250 or 100 data points (about 40 or 16 hours). Production rate increases with [**Delay**] due to possible undesired reactions between circuit components.

SI 5: Multiplex Timer Experiments (Systems 1 and 2)

Multiplexing experiments were conducted the same as the experiments described in SI 3-4. Briefly, the **Reporters** of each system were mixed and a baseline was taken followed by the addition of **Delay** and **Source** complexes. **Initiator** was added after 22-24 hours. For experiments comparing data of each system in isolation *vs*. together, the reaction solution contained **Reporters** from both systems, but only the **D**, **S** and **I** from the system being studied (dashed lines in Supp. Fig. 16). System 1 was tracked using FAM and System 2 with TexasRed fluorophores using two different filters on the qPCR. Fluorescence from one fluorophore was not observed when measuring the fluorescence of the other fluorophore.

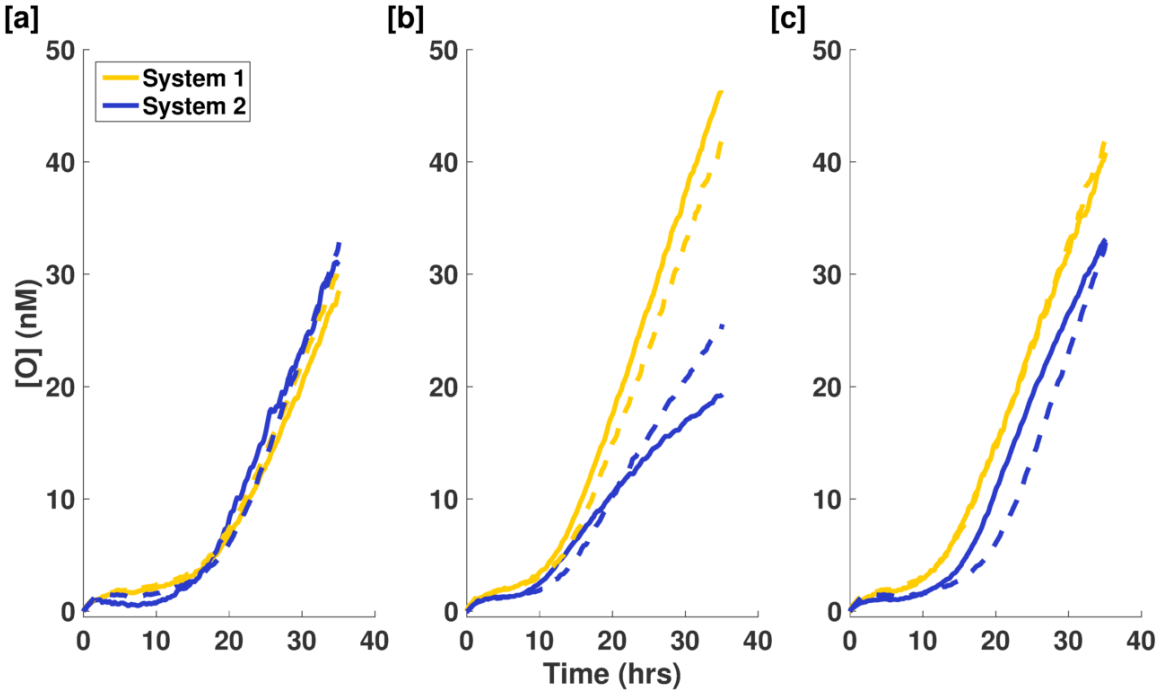

Supplemental Figure 16: Additional examples of multiplexing two timer circuits. In each case, dashed lines indicate a reaction with the system in isolation. (a) Reaction mixture conditions were chosen such that both systems would release their respective O at the same time (19 hours) and rate. $[\mathbf{S}]_0=[\mathbf{I}]_0=1$ μM; $\{[\mathbf{D}]_{Sys1}, [\mathbf{D}]_{Sys2}\}=\{130$ nM, 165 nM$\}$. (b) The release rate of each system can be independently controlled while keeping the delay time constant (9 hours). $[\mathbf{S}]_0=[\mathbf{I}]_0=1$ μM for Sys1 and 0.5 μM for Sys2; $\{[\mathbf{D}]_{Sys1}, [\mathbf{D}]_{Sys2}\}=\{100$ nM, 50 nM$\}$. (c) The time of release (9 and 19 hours) of each system can be independently controlled while keeping the release rate constant. $[\mathbf{S}]_0=[\mathbf{I}]_0=1$ μM; $\{[\mathbf{D}]_{Sys1}, [\mathbf{D}]_{Sys2}\}=\{100$ nM, 165 nM$\}$.

SI 6: Timer Circuit Simulations and Characterization of Leak Reactions

Since the DNA strand-displacement circuit can be represented by a series of mathematical equations (SI-Equations 1 and 5 and SI Figure 6), a model that matches the experimental behavior of the system could be built to further tune the circuit for future applications. However, we found that a simple model derived from those equations failed to quantitatively capture the delay times observed in experiments (Supp. Figure 17). Based on that mismatch and the observation of an increase in fluorescence (or detected **O**) by the **Reporter** when **S** is added in the absence of **I** or **D** (Supp. Figure 4), we postulated that a series of interactions might exist between **S**, **D**, **I** and **Reporter** beyond what is predicted by the simple model.

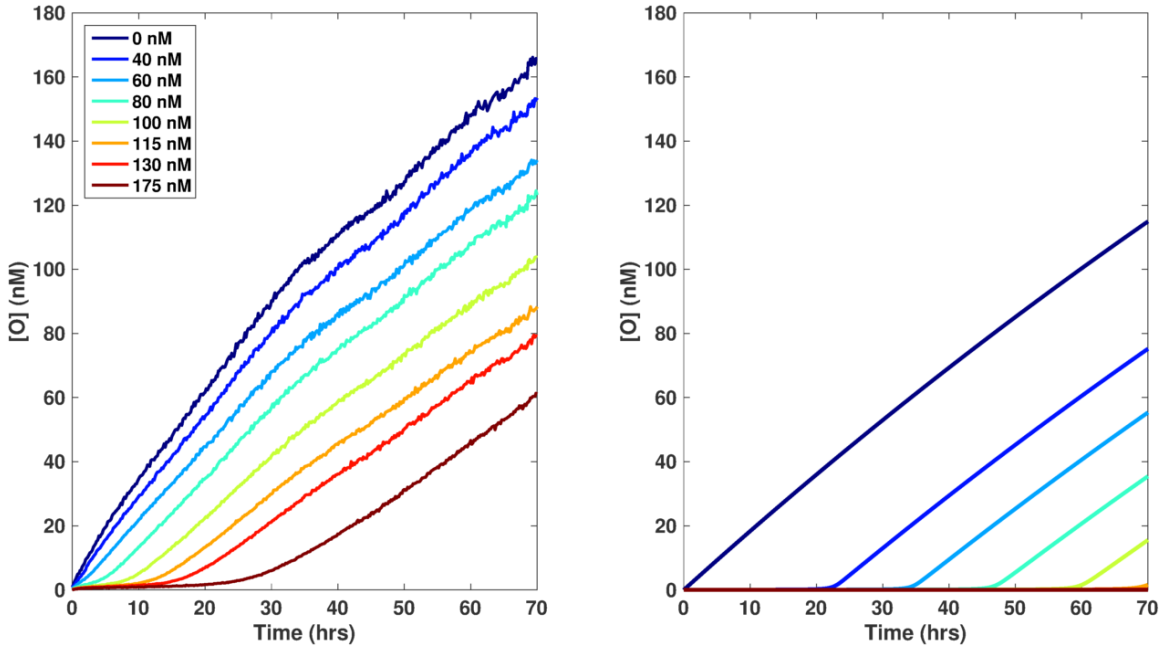

Supplemental Figure 17: Comparison of data (left) and a model considering only abstract reactions described in SI-Eqn. 5 and Supp. Fig. 6 (right) for System 1 using 1 µM **S** and **I**. **Delay** concentrations for both plots are shown in the legend. Parameters for the model were as described in SI 2 (Supp. Figs. 3,6) and in Zhang and Winfree.[4] Note the decrease in overall production and increase in time delay of the model prediction compared to experimental results.

In control experiments, we found that mixing the **Reporter** and **Source** quickly produced an observable fluorescence signal in the absence of **Initiator** (Supp. Fig. 4), suggesting that the **Source** complex and the **Reporter** interacted in an undesired or "leak" reaction (Supp. Fig. 18a). While by design these species could interact through a 4-way 0bp pair branch migration interaction, such a pathway would not explain the fast rate of reaction we observed. We therefore postulated that this reaction could be due to truncations or base mismatches within the toehold region of the bottom strand of some **S** complexes. We designated **S** complexes with these variations as the subspecies $\mathbf{S}_{\mathbf{Leak}}$. These complexes would not have been separated from pure **S** complex during the purification process because their electrophoretic mobility is very similar to that of **S**.

We also observed that some leftover **O** remained after the gel purification process due to the proximity of the bands in the gel. Purifying **S** using a 15% polyacrylamide gel instead of a 10% gel significantly reduced the level of pre-initiation **O** detected, but some may still remain in the purified **S** complex solution. The leftover **O** and $\mathbf{S_{Leak}}$ complex are also expected to interact with the **Delay** complex for timer circuit reactions. We also considered a leak reaction between the **Initiator** and the **Delay** complex since there are 7 complementary nucleotides for a transient hybridization. The schematic shown in Supp. Figures 18-20 shows the possible leak reactions considered here. Unless specified in the figure captions, reaction rate constants for these reactions were taken from Supplemental Reference 4 or fit using the bimolecular rate equation shown in SI 2 and Supp. Figure 5. This approach of choosing reaction rate constants supports a physical representation of the postulated reactions and provides consistency with studies of other DNA strand-displacement reactions.

While the reactions described above may account for the unintended reactions that occurred within the timer system, including these reactions in a model still predicted significantly different time delay values than what were observed experimentally. To account for the decreased time delay observed in experiments, we added a small leak reaction between pure **Source** complexes and **Delay** complexes. While such a reaction would be expected to occur with a rate constant smaller than k_{0bp}, a reaction rate constant of k_{1bp} was needed to account for the large decrease in delay time. As noted in SI 2, we found that a reaction between $\mathbf{S_{Leak}}$ and **I** produced a better fit to the production dynamics. However, we would not expect this reaction to occur since **S** and **I** are incubated prior to PAGE purification of the **S** complex, any **S** species that would quickly react with **I** would be removed. Supp. Figure 19 shows an example comparison between experimental data (System 1, [**S**]=[**I**]=1 μM) and the resulting model prediction. While these reactions are only a possible description of the interactions between the DNA species, they show that an understanding of the reaction behavior is possible through the incorporation of leak pathways. We found that incorporation of each of these leak pathways into our model, using previously published rates and the fitted parameters of [$\mathbf{S_{Leak}}$], $k_{S,Leak}$ and k_{0bp} as described in SI 2 (no additional fitting parameters were required) produced quantitative agreement between our model and the experimental results that we observed (Supp. Fig. 21). Thus, we expect that this model can be used to tune the system's performance, including release rates and delay times.

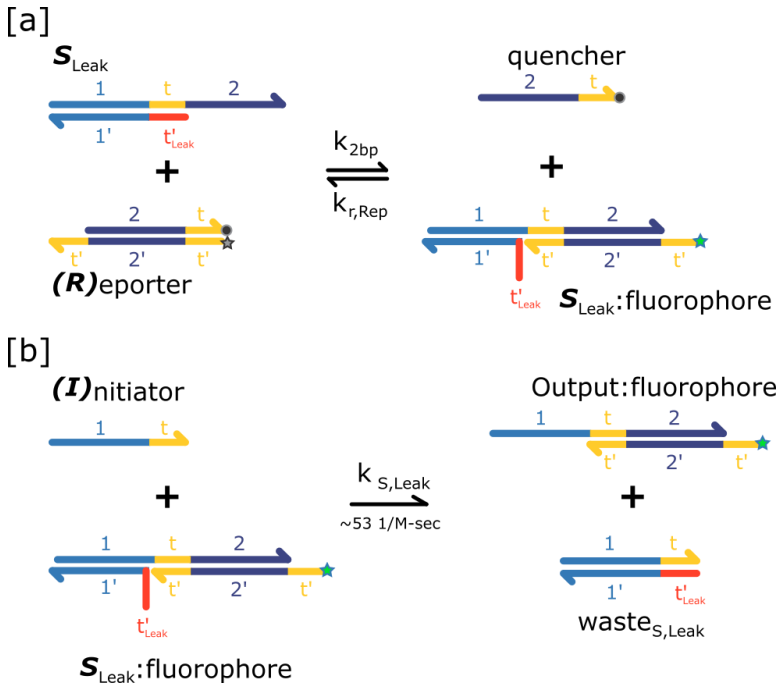

Supplemental Figure 18: Reactions between a **Source** complex with mismatches or base truncations in the toehold region and the **Reporter** complex lead to the detection of a fluorescent signal prior to the addition of the **Initiator**. (a) **S_{Leak}** complex interacts reversibly with the **Reporter** to produce a fluorescent complex that reacts irreversibly with the **Initiator** (b). $k_{r,rep}$ was calculated from k_{5bp} (ref. 4) and the experimentally measured K_{eq} of the **Reporter-Output** reaction (Supp. Fig. 2).

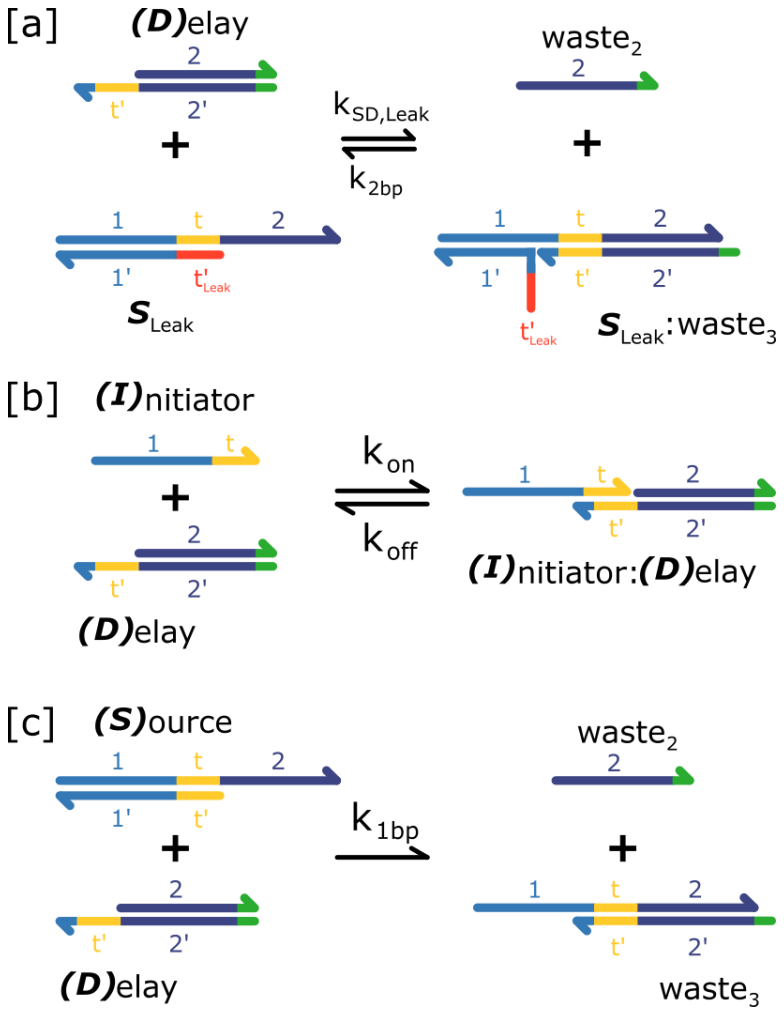

Supplemental Figure 19: Reactions between the **Delay** complex and other reaction species. (a) **Delay** and $\mathbf{S_{Leak}}$ react reversibly with a forward rate constant estimated to be $k_{SD,Leak}$ ~250 1/M-sec. (b) **Initiator** hybridizes and de-hybridizes with the toehold of the **Delay** complex. From Zhang and Winfree,[4] k_{on} ~ 3.5x10^6 1/M-sec and k_{off} ~ 0.08 1/sec. (c) Leak reaction between pure **Source** complex and the **Delay** complex.

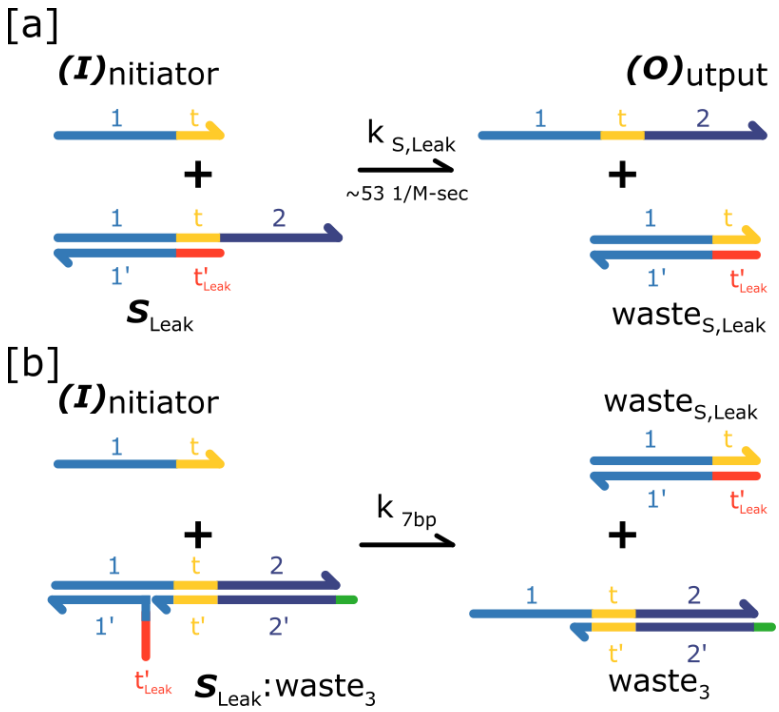

Supplemental Figure 20: Leak reactions with **Initiator**. (a) Reaction between **I** and $\mathbf{S_{Leak}}$. (b) Reaction between **I** and the complex produced from $\mathbf{S_{Leak}}$+**D**.

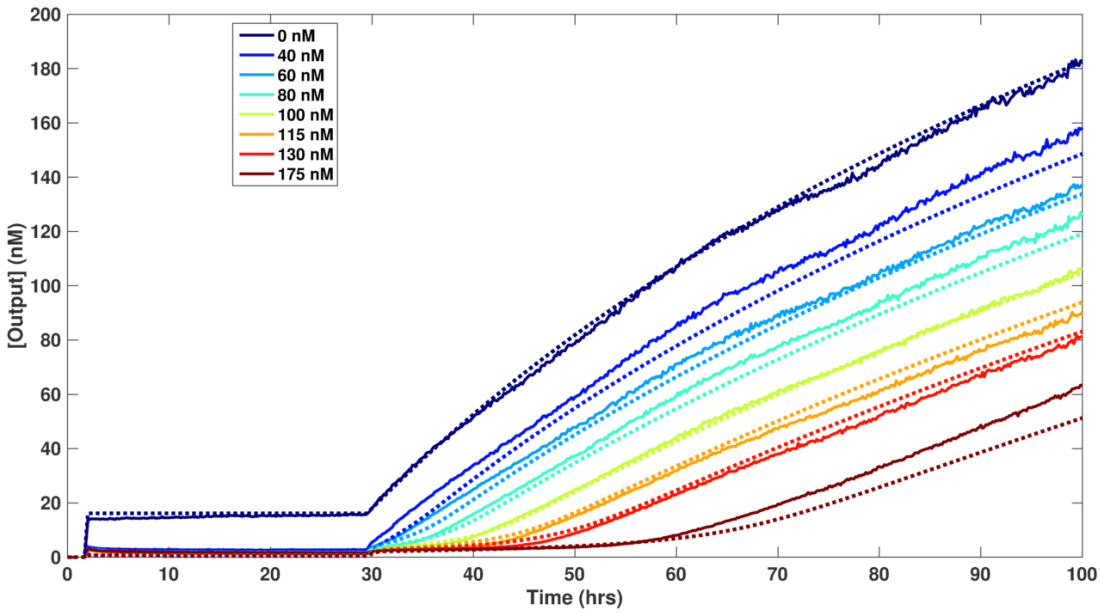

Supplemental Figure 21: Comparison of data and the model prediction for System 1 using 1 μM **S** and **I**. **Delay** concentrations are listed in the legend. Reporter-only baseline was initially measured followed by **Source** and **Delay** complex addition at 1 hour. **Initiator** was added after 30 hours. Parameters and reactions included in the model were as described above in Supp. Figs. 18-20 and in Zhang and Winfree.[4]

Supplemental References

1. Qian, L.; Winfree, E. (2011) "Scaling up digital circuit computation with DNA strand displacement cascades." *Science*, *332.6034*, 1196-1201.
2. Zadeh J., Steenberg C., Bois J., Wolfe B., Pierce M., Khan A., Dirks R., Pierce N. (2011) "NUPACK: analysis and design of nucleic acid systems." *Journal of Computational Chemistry*, 32(1):170-173.
3. Puglisi, J. D.; Tinoco, I. Jr. (1989) "Absorbance Melting Curves of RNA." *Methods in Enzymol.*, *180,* 304–325.
4. Zhang, D. Y.; Winfree, E. (2009) "Control of DNA strand displacement kinetics using toehold exchange." *J. Am. Chem. Soc.*, *131.47*, 17303-17314.